



# Electric field processing to control the structure of poly(vinylidene fluoride) composite proton conducting membranes

D. Liu, M.Z. Yates \*

Department of Chemical Engineering and Laboratory for Laser Energetics, University of Rochester, Rochester, NY 14627, United States

## ARTICLE INFO

### Article history:

Received 27 June 2008

Received in revised form 29 August 2008

Accepted 18 October 2008

Available online 5 November 2008

### Keywords:

Nafion

ZrPSPP

PVdF

Electric field processing

Fuel cell membrane

## ABSTRACT

A novel method is reported for controlling the structure of poly(vinylidene fluoride) (PVdF) composite proton conducting membranes. When proton conducting Nafion or zirconium phosphate sulfophenylphosphonate (ZrPSPP) particles are dispersed in a mixed colloidal suspension with PVdF particles, the proton conducting particles selectively respond to an applied electric field. Under appropriate conditions, the proton conducting particles are induced to assemble into chains that rapidly grow to span the gap between electrodes as the electric field is applied. By removing the solvent and melting the PVdF phase while applying the electric field, composite membranes were formed that have field-induced structure. In comparison to randomly structured composites, the electric field-processed Nafion/PVdF or ZrPSPP/PVdF composite membranes showed improved proton conductivity, water sorption, selectivity for protons over methanol, and controlled surface area changes upon swelling with water. The transport and mechanical properties of the electric field-processed composite membranes suggest the potential for improved performance in direct methanol fuel cells.

© 2008 Elsevier B.V. All rights reserved.

## 1. Introduction

Fuel cells operating directly on methanol are attractive for portable power and vehicular applications because the high-energy density liquid methanol fuel can be easily stored and handled at atmospheric pressure and used without fuel reforming [1,2]. One of the main technical challenges limiting direct methanol fuel cell (DMFC) commercialization is membrane performance. Polymeric perfluorinated ionomers such as Nafion are the most commonly used proton exchange membranes in fuel cells due to their good electrochemical stability and high proton conductivity that serve as benchmarks for membrane performance [3,4]. However, Nafion and related materials suffer from unacceptably high methanol permeability that limits performance in DMFCs due to fuel crossover from the anode to the cathode [5]. The permeability of Nafion to methanol is directly related to the high swelling of Nafion by water, since water and methanol are transported together [3,6]. Dry membranes are much less conductive because protons are transported through Nafion and similar materials primarily as  $\text{H}_3\text{O}^+$  ions [7]. As a result, water sorption into the membranes is required for conductivity. Unfortunately, the dimensional changes that accompany water swelling can cause fuel cell device failure

as mechanical stress leads to detachment of electrodes from the membrane [8,9]. It remains a significant challenge to design durable membranes for DMFCs that maintain high proton conductivity while limiting methanol permeability and controlling membrane swelling.

One route to enhance the mechanical and transport properties of DMFC membranes is through the use of polymer composites. Small particles that are impermeable to methanol can be added to proton conducting polymers to form composite membranes with reduced water swelling and decreased methanol permeation. Often the methanol impermeable particles lower the proton conductivity and methanol permeability simultaneously, limiting membrane performance [10,11]. Alternatively, proton conducting composites with reduced methanol permeation may be formed from a methanol impermeable polymer support matrix containing dispersed proton conducting particles. For example, zirconium phosphate sulfophenylphosphonate (ZrPSPP) particles have high proton conductivity similar to that of conventional polymer electrolytes and are thermally stable up to 200 °C [12–14]. Composite membranes consisting of a nonconductive polymer loaded with ZrPSPP particles will have high proton conductivity if the loading of ZrPSPP is high enough for the particles to form an interconnected network for proton transport. Usually the high particle loading required for conductivity is detrimental to the mechanical stability of the membrane [15,16].

The goal of the present study is to engineer composite membrane structure to optimize performance and minimize the amount

\* Corresponding author. Tel.: +1 585 273 2335; fax: +1 585 273 1348.

E-mail address: [myates@che.rochester.edu](mailto:myates@che.rochester.edu) (M.Z. Yates).

of proton conductive particles required. The conductivity and permeability of composite membranes depend strongly not only on the concentration of functional particles, but also the spatial arrangement of particles within the membrane. Other researchers have shown that the manipulation of the distribution of functional particles within a polymeric matrix can enhance the membrane properties [17–19]. In the present study, electric fields are applied during membrane formation to control the composite membrane structure. When an electric field is applied to a particle suspension, it can cause particles to aggregate into chains aligned in the direction of the applied field [20,21]. Solidification induced by chemical reaction or physical removal of solvent can convert the particle suspension into a solid composite membrane with a fixed field-induced structure. A previous study has demonstrated that electric field-induced chaining of conductive particles can enhance the proton conductivity of composite silicone membranes in the direction of the applied field [22]. In the previous study, chaining of proton conducting particles was carried out in a polymerizable liquid silicone. However, silicone polymers are not suitable for fuel cell membranes due to high oxygen permeability, and common membrane materials promising for fuel cell application are not available as polymerizable liquids. Here we report a novel method to control composite membrane structure by selectively forming proton conducting particle chains from mixed colloidal suspensions of conductive and nonconductive particles. This new technique is used to control the structure of composite proton conducting membranes based on poly(vinylidene fluoride) (PVdF), a polymer with excellent barrier properties for methanol and that is chemically and mechanically stable under fuel cell operating conditions. When blended with proton conducting ionomers such as Nafion, PVdF membranes have shown promising performance in DMFCs [23–26]. Electric field processing offers a potential route to enhance PVdF composite membrane performance in DMFCs.

## 2. Experimental

### 2.1. Materials

PVdF ( $M_w = 534,000$  g/mol,  $m_p = 165^\circ\text{C}$ ) was purchased from Sigma–Aldrich. Nafion 1100 dispersion (Dupont DE2021) was obtained from Ion Power Inc. Fluorolink C (Fomblin, fluorocarbon oil) was purchased from Solvay Solexis. ZrPSPP was produced following a method reported in the literature [27]. First, metasulphophenylphosphonic acid ( $\text{H}_2\text{SPP}$ ) was synthesized as described in the literature [28]. Next, ZrPSPP was prepared by mixing a solution of  $0.16\text{ M ZrOCl}_2 \cdot 8\text{H}_2\text{O}$  and  $1\text{ M HF}$  with a solution of  $0.1\text{ M H}_3\text{PO}_4$ ,  $0.1\text{ M H}_2\text{SPP}$ , and  $1\text{ M HCl}$  with a molar ratio of  $(\text{H}_3\text{PO}_4 + \text{H}_2\text{SPP})/\text{Zr} = 2.5$ . Then the product was washed and dried as described in the literature [27]. The general formula of the as-obtained ZrPSPP is  $\text{Zr}(\text{HPO}_4)_{1.00}(\text{SPP})_{1.00} \cdot n\text{H}_2\text{O}$ , with  $\text{SPP} = \text{O}_3\text{PC}_6\text{H}_4\text{SO}_3\text{H}$ .

### 2.2. Particle preparation

The Nafion 1100 dispersion was placed in a rotary vacuum evaporator (Büchi Rotavapor R-200, Brinkmann Instruments Inc.) at  $70^\circ\text{C}$  and *ca.*  $15\text{ mmHg}$  till a viscous solid residue was obtained. The viscous residue was transferred to a vacuum oven maintained at room temperature until dry. The vacuum dried Nafion was then frozen with liquid nitrogen, ground with a pestle and mortar, and sieved to produce particles less than  $45\text{ }\mu\text{m}$ . Micron-sized ZrPSPP particles were prepared through an electrospray process. A  $1.5\text{ wt\%}$  suspension of ZrPSPP in a mixture of deionized water and NMP (volume ratio of water to NMP =  $1:20$ ) was injected into a stainless steel needle (22 gauge) using a syringe pump (Pump 11, Harvard Apparatus). The needle was maintained at  $5\text{ kV/cm}$  DC potential above a grounded aluminum plate. The ZrPSPP particles were collected and dried on the aluminum plate maintained at  $160^\circ\text{C}$ . PVdF

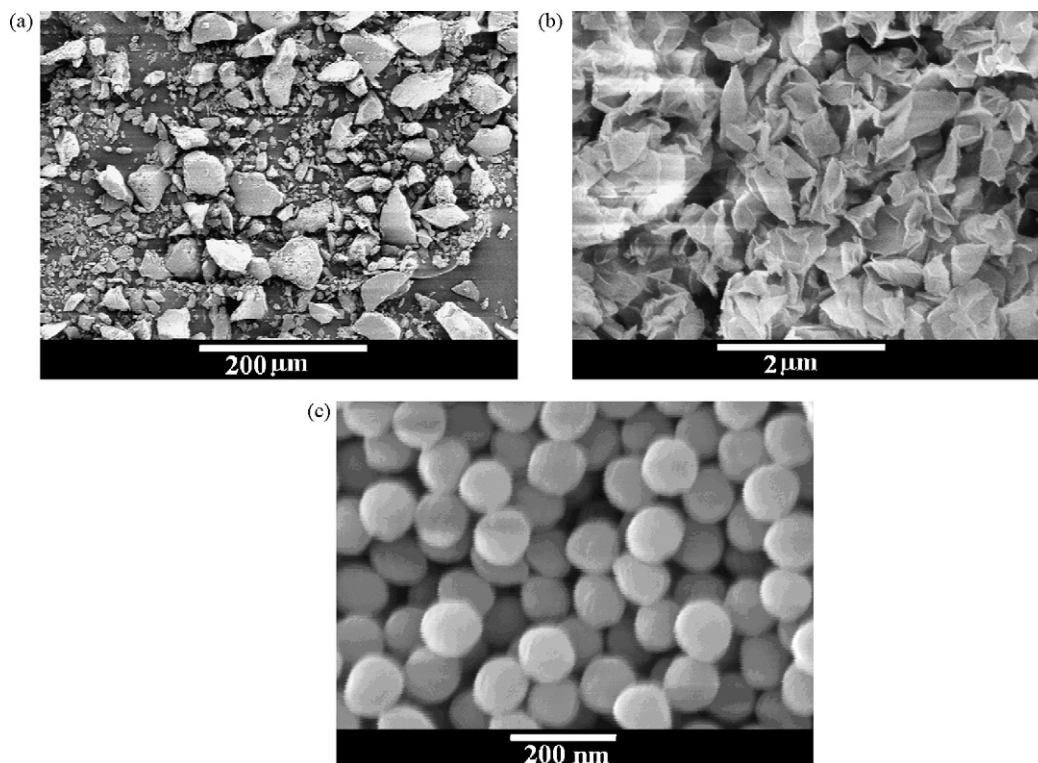


Fig. 1. SEM images of (a) Nafion, (b) ZrPSPP and (c) PVdF particles used in fabrication of Nafion/PVdF and ZrPSPP/PVdF composite membranes under an applied electric field.

was in the form of a fine powder and used as received. Fig. 1(a)–(c) shows the morphology of the Nafion, ZrPSPP and PVdF particles, respectively, used in the experiments. The dielectric constant and conductivity of these particles were measured using an impedance gain phase analyzer (Solartron 1260, Solartron Analytical) with a sample holder for solid materials (1296 2A, Solartron Analytical). The particles were pressed into a pellet with diameter of 2 cm and thickness of  $\sim 300\ \mu\text{m}$ . The sample holder consists of two parallel electrodes that contact each side of the sample pellet to form a parallel capacitor. The impedance gain phase analyzer with a sinusoidal test signal was used to analyze the output impedance signal after interaction with the sample. Using the output signals of capacitance and resistance in the measurement, the dielectric constant and conductivity of the samples were calculated.

### 2.3. Experimental set-up

Fig. 2 shows the device used to fabricate composite PVdF membranes under an applied electric field. The cell consists of a “U”-shaped Teflon frame sandwiched between two aluminum electrodes. Teflon plates held outside the electrodes act as electrical insulation. The five pieces were clamped together to form a cell with dimensions of  $2.5\ \text{cm} \times 2.5\ \text{cm} \times 800\ \mu\text{m}$ . Temperature of the cell was controlled by a heating mantle. The electric field applied to the cell electrodes could be controlled from 0 to 10 kV peak to peak with frequency in the range of 0–20 MHz by passing the output signal of a function/arbitrary waveform generator (Agilent Model 33220A) through a high voltage amplifier (Trek Model 10/10B).

### 2.4. Membrane preparation

Nafion or ZrPSPP particles and PVdF particles were dispersed using a Vortex-Genie™ mixer (Scientific Industries Inc.) to form a suspension with 30 wt% total solids in Fomblin fluorocarbon oil. The suspension was transferred to the electrode cell, exposed to the electric field at room temperature, and then heated to  $170^\circ\text{C}$  in the heating mantle to melt PVdF while maintaining the electric field. The composite was then pressed together with a thin piece of Teflon plate. Finally, the cell was cooled to room temperature as the electric field and the pressure from Teflon were continuously applied.

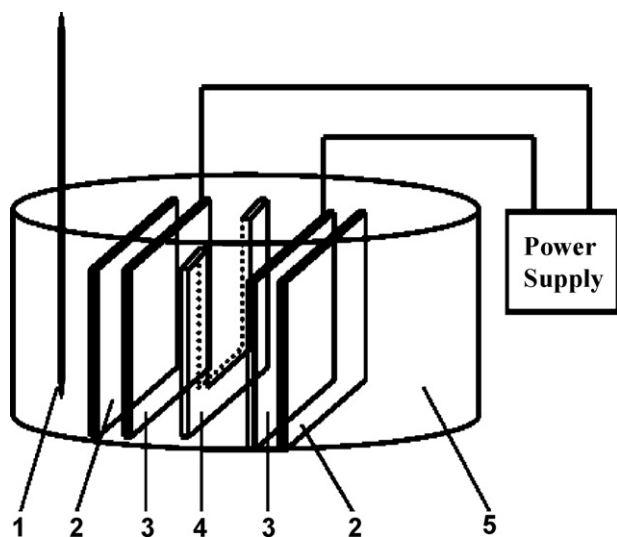


Fig. 2. Apparatus for assembling Nafion/PVdF and ZrPSPP/PVdF composites: (1) thermocouple, (2) insulating Teflon plate, (3) aluminum electrode, (4) “U”-shaped thin Teflon, and (5) heating mantle. Pieces 2, 3, and 4 were clamped together and the membrane was formed between the electrodes inside the thin “U”-shaped opening.

The dimensions of the as-fabricated composite membrane are the same as the cell dimensions of  $2.5\ \text{cm} \times 2.5\ \text{cm} \times 800\ \mu\text{m}$ . The composite membrane was transferred to a pressure vessel and liquid  $\text{CO}_2$  was used to extract the residual fluorocarbon oil. Extraction was carried out for 3 h using  $\text{CO}_2$  at 155 bar and room temperature flowing at a rate of 0.5 ml/min. In control experiments, composite membranes with randomly distributed particles were prepared with the same procedure except for the application of the electric field.

### 2.5. Membrane characterization

An inverted phase contrast optical microscope was used to observe the response of Nafion and ZrPSPP particles to the electric field. The particle morphology and the membrane surface morphology were examined with scanning electron microscopy (LEO 982 FE-SEM). Proton conductivity measurements of the membranes were carried out at room temperature using two-point probe alternating current (AC) impedance spectroscopy (EIS 300, Gamry Instruments) over a frequency range of 300 kHz to 0.1 Hz. Prior to the conductivity measurement, all membranes were submerged in deionized water at room temperature for at least 2 days to reach saturation.

Water sorption of the composite membranes was determined by the percentage weight difference between the dry and fully saturated states. The dry state was defined as the weight of the membrane ( $W_{\text{dry}}$ ) after 24 h under vacuum at  $70^\circ\text{C}$ . The fully saturated state was defined as the weight of the membranes ( $W_{\text{wet}}$ ) after submersion in deionized water at room temperature for 2 days. The water sorption of the membranes was calculated by  $(W_{\text{wet}} - W_{\text{dry}})/W_{\text{dry}} \times 100\%$ . A micrometer was used to measure the percentage change in membrane area between the dry and fully hydrated states.

Methanol permeability of the membranes was investigated using an in-house constructed glass permeability cell. The membrane was clamped between two vessels, each with a volume of 30 ml. At the beginning of the methanol permeation test, vessel 1 was filled with 3 M aqueous methanol solution and vessel 2 was filled with deionized water. The apparatus was kept at room temperature ( $\sim 26^\circ\text{C}$ ) under magnetic stirring at rate of 1200 rpm while measuring the methanol concentration of vessel 2 versus time using a gas chromatograph (Hewlett Packard model 8590A) with a capillary column (Agilent Co., DB-Wax,  $30\ \text{m} \times 0.32\ \text{mm} \times 0.50\ \mu\text{m}$ ). The methanol permeability was determined from the measured concentration versus time by using an approximate solution of the continuity equation for diffusion in plane sheet geometry at early times [29,30].

A Pyris Diamond Thermomechanical Analyzer (PerkinElmer Inc.) was used to carry out tensile tests of membranes. Test specimens of composite membranes were 2 mm in width and  $\sim 800\ \mu\text{m}$  in thickness. A pure PVdF specimen with 2 mm width and  $\sim 200\ \mu\text{m}$  in thickness was cut from a solvent-cast film. The grip distance was 10 mm and the cross-head speed was 25 mm/min. The strength and tensile elongation at rupture of the membranes were obtained from stress–strain curves.

## 3. Results and discussion

### 3.1. Response of particles to an applied electric field

When particles are suspended in solvents and exposed to an electric field, the field induces polarization of the particles due to the mismatch in permittivity or conductivity between particles and solvent. Interaction between polarized particles can cause them to

**Table 1**

Properties of particles and solvent used in fabrication of composite Nafion/PVdF and ZrPSPP/PVdF membranes.

Name	Shape	Size ( $\mu\text{m}$ ) radius	$\varepsilon_i$ (1000 Hz)	$\sigma_i$ (S/m)	$\beta$	$E$ (V/mm) ( $\lambda \geq 1$ ) $T = 25^\circ\text{C}$	$E$ (V/mm) ( $\lambda \geq 1$ ) $T = 170^\circ\text{C}$
Nafion	Irregular	$\sim 11$	10,000	$10^0$	$\sim 1$	0.23	0.28
ZrPSPP	Irregular	$\sim 1$	10,000	$10^0$	$\sim 1$	8.39	10.23
PVdF	Spherical	$\sim 0.05$	7.72	$10^{-12}$	$\sim 0.48$	1578	1926
Fluorolink C	–	–	2.10	$10^{-12}$	–	–	–

aggregate into chains aligned in the direction of the applied field. For colloidal-sized particles, Brownian motion acts to disrupt the alignment induced by the electric field [31]. Particle alignment occurs only when the field-induced particle dipole interactions dominate Brownian motion. For a spherical particle, the parameter defining the relative strengths of the polarization forces and Brownian motion is [32,33]:

$$\lambda = \frac{\pi \varepsilon_0 \varepsilon_1 r^3 (\beta E)^2}{K_B T} \quad (1)$$

where  $\varepsilon_0$  is the permittivity of free space,  $\varepsilon_1$  is the relative dielectric constant of the solvent,  $r$  is the radius of the particle,  $E$  is the applied field strength,  $K_B$  is the Boltzmann's constant, and  $T$  is the absolute temperature.  $\beta$  represents the particle dipole coefficient, given under our experimental conditions by  $(\sigma_2 - \sigma_1)/(\sigma_2 + 2\sigma_1)$ , where  $\sigma_1$  and  $\sigma_2$  are the conductivity of the solvent and particle, respectively [20,34]. When  $\lambda$  calculated by Eq. (1) is greater than 1, the electric field induced polarization forces dominate Brownian motion and field induced particle structuring is predicted.

To simplify the analysis of the present system, all particles were assumed to be spheres with an average radius of 11  $\mu\text{m}$  for Nafion, 1  $\mu\text{m}$  for ZrPSPP and 50 nm for PVdF on the basis of the approximate average sizes measured by SEM. The dielectric constant and conductivity of these particles were measured as shown in Table 1. The minimum field strength ( $E$ ) required to align particles can be estimated from Eq. (1) using the data in Table 1. The calculated

minimum field strengths required to align the Nafion, ZrPSPP, and PVdF particles at room temperature are 0.23 V/mm, 8.39 V/mm, and 1578 V/mm, respectively. When the temperature is raised to 170  $^\circ\text{C}$ , the minimum field strengths are increased to 0.28 V/mm, 10.23 V/mm, and 1926 V/mm, respectively. Therefore, the calculation predicts that both Nafion and ZrPSPP particles will respond to the electric field at much lower field strength than required for PVdF. In the experiment, a mixed colloidal suspension of proton conducting particles (either Nafion or ZrPSPP) and PVdF particles was formed. The experimental AC field strength was chosen to selectively align the proton conducting particles, while leaving the PVdF particles unaffected. Field strengths of 100 V/mm ( $f = 25$  Hz) and 500 V/mm ( $f = 100$  Hz) were chosen to align the Nafion and ZrPSPP particles, respectively.

The response of the particles to the applied field was observed directly at room temperature with an optical microscope. Fig. 3(a) and (b) shows a suspension of 2.5 wt% Nafion and 2.5 wt% PVdF in Fomblin oil. In Fig. 3(a), the large-sized Nafion and small sized PVdF are observed to be distributed randomly before the electric field was applied. Upon applying an electric field of 100 V/mm at 25 Hz, the Nafion particles rapidly form chains. The PVdF particles are unaffected by the electric field and are observed to be pushed aside by the growing Nafion particle chains. The Nafion particle chains extend in the direction of the applied field and completely bridge the gap between the two electrodes, as illustrated in Fig. 3(b). Similar phenomena were observed for a suspension of 2.5 wt% ZrPSPP

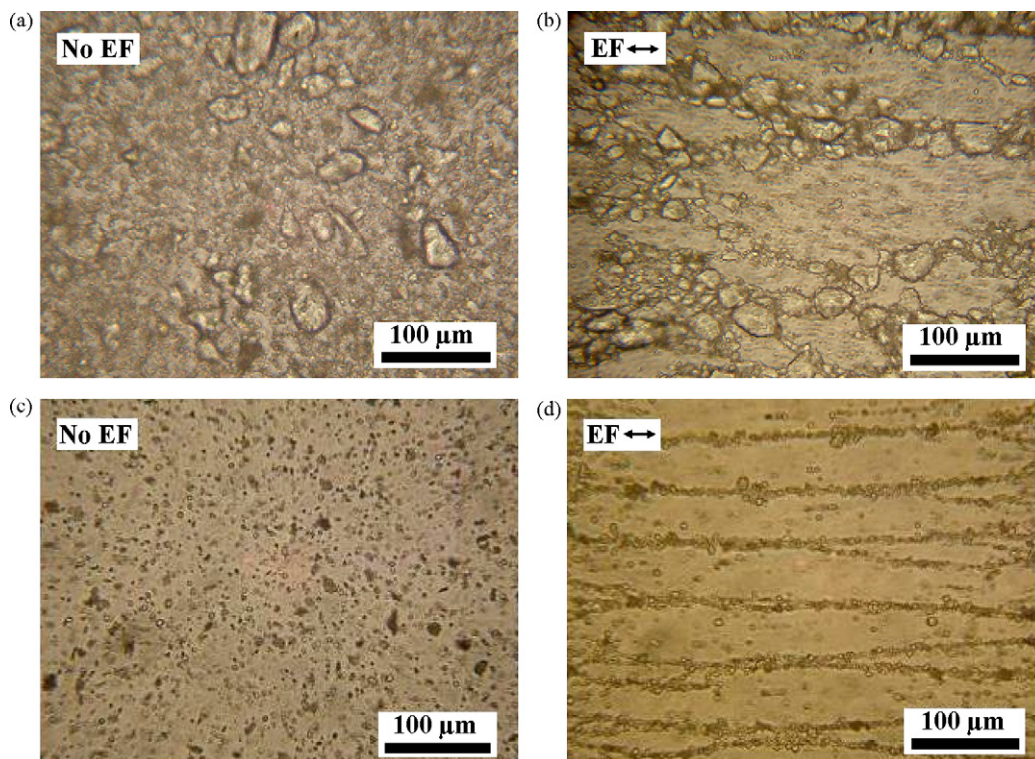


**Fig. 3.** Microscopic images showing the response of particles in Fomblin oil suspension to an applied electric field: (a) Nafion/PVdF suspension before and (b) after exposure to the electric field. (c) ZrPSPP/PVdF suspension before and (d) after exposure to the electric field.

and 2.5 wt% PVdF in Fomblin oil, as shown in Fig. 3(c) and (d), when a field of 500 V/mm at 100 Hz was applied. The visual observation clearly shows the proton conducting particles are induced to form continuous chains bridging the gap between the electrodes while the nonconductive PVdF particles remain randomly distributed in the suspension in Fomblin oil. The selective response of proton conducting particles is the basis for forming PVdF composites of controlled structure. Membranes are formed by removing the solvent at high temperature and melting the PVdF particles together to form a supporting matrix around the proton conducting particle chains.

### 3.2. Morphology of Nafion/PVdF and ZrPSPP/PVdF membranes

Fig. 4(a)–(d) shows the surface morphology of composite membranes formed with and without an applied electric field after extracting the residual fluorocarbon oil. The Nafion/PVdF membrane has a smooth and homogenous surface when it is prepared without the electric field, as shown in Fig. 4(a). The membrane sur-

face appears less homogenous and rough, as shown in Fig. 4(b), when prepared under the applied electric field. The changes in surface morphology are suggestive of field-induced changes in the morphology of the Nafion and PVdF phases. However, it is not possible to differentiate phase boundaries from the SEM images since Nafion and PVdF are melted together. A side-view image of a 20 wt% Nafion/PVdF composite membrane is in Fig. 4(e) that clearly shows the Nafion particle chains are intact along the electric field direction. The sample shown in Fig. 4(e) was processed at a lower temperature (approximately 160 °C) to enhance visualization of Nafion chains by reducing blending of the two phases.

In contrast to the Nafion/PVdF composites, separate phases are easily observed in SEM images of ZrPSPP/PVdF composites (Fig. 4(c) and (d)). The ZrPSPP particle aggregates are clearly separated from the surrounding PVdF matrix. These voids are possibly due to the extraction of fluorocarbon oil, but more likely due to phase separation between ZrPSPP and PVdF since no voids are visible with Nafion/PVdF membranes processed at 170 °C. Fig. 4(c) shows the membrane formed without the applied electric field. The ZrP-

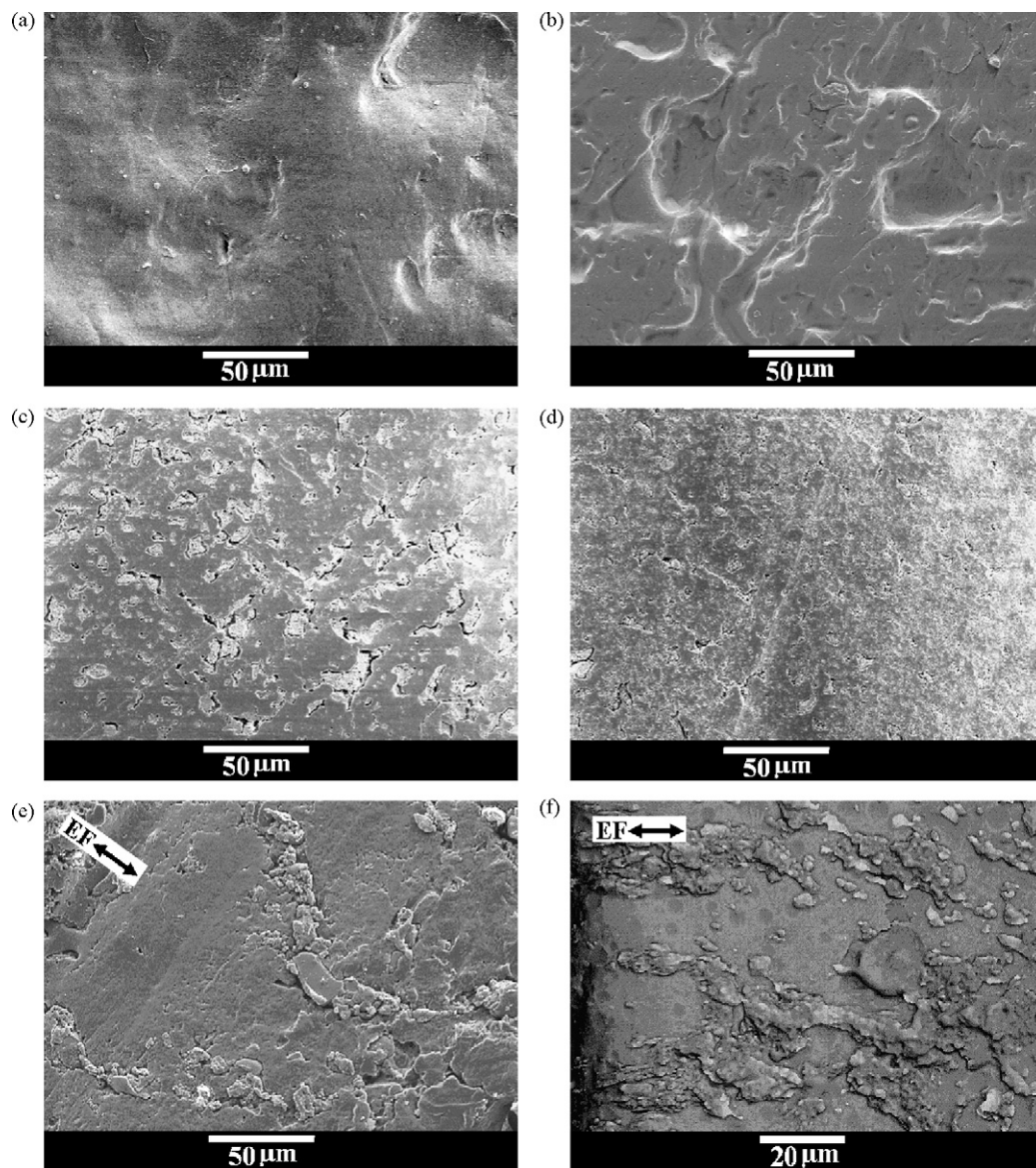


**Fig. 4.** SEM images showing top-view surface morphology of 20 wt% Nafion/PVdF film prepared (a) without and (b) with an electric field and 20 wt% ZrPSPP/PVdF film prepared (c) without and (d) with an applied field. Images (e) and (f) show the side-view morphology of 20 wt% Nafion/PVdF and 20 wt% ZrPSPP/PVdF composite films, respectively.

SPP/PVdF composite membranes prepared under the electric field appear to have smaller ZrPSPP domains at the surface, as shown in Fig. 4(d). The SEM images only show the phase domains at the surface and provide no information on the distribution of particles through the membrane thickness. The apparently lower number of aggregates at the surface when the electric field is applied may be due to the field-induced particle chaining across the membrane. It is possible that the particle concentration and aggregation at the surface of the membrane may be enhanced by attraction between the ZrPSPP particles and electrode surface. These images suggest that the electric field induced forces reduce particle aggregation in the lateral direction across the surface of the membrane, while enhancing aggregation in the field direction. As a result, the apparent concentration at the surface appears higher when no field is applied to the composite membranes. Fig. 4(f) shows the side-view image of the ZrPSPP/PVdF film prepared through the experiment. Particle chains are visible along the field direction in the final membrane.

### 3.3. Tensile testing

For a pure PVdF film, the measured maximum strength and elongation at break were 37 MPa and 260%, respectively. The electric field-processed composite membranes have a lower maximum break strength and elongation than pure PVdF. For example, a 10-wt% Nafion/PVdF membrane processed under electric field had maximum break strength and elongation of 20 MPa and 120%, respectively. The reduced mechanical strength of the composites is a result of weak interfacial adhesion between the proton conductive and PVdF phases that does not allow stress to be efficiently transferred from one phase to another during yielding or fracture processes. The electric field induced particle chaining enhances aggregation of the proton conducting phase across the membrane thickness. While the particle chaining can enhance transport properties, it can adversely affect membrane strength.

### 3.4. Water sorption

The percent increase in weight of the membranes due to water sorption is shown in Fig. 5(a)–(b). For Nafion/PVdF membranes, the water sorption increases with increasing Nafion content in both aligned and non-aligned composite membranes. Considering that the PVdF is hydrophobic and has zero water sorption on its own, all absorbed water is due to the presence of Nafion particles. The membranes prepared with an applied field have higher water uptake than those with the same Nafion content that are formed without the electric field. The membranes formed without the electric field likely have some Nafion domains that are completely surrounded by PVdF and thus inaccessible to water. The particle chaining induced by the electric field brings the Nafion particles into good contact. As a result, more Nafion particles are accessible to water and the electric field-processed membranes display increased water sorption.

A similar water sorption tendency was observed for ZrPSPP/PVdF composite membranes, as shown in Fig. 5(b). The water uptake is directly proportional to ZrPSPP particle concentration in the composite membranes. As with Nafion, the electric field induced particle chaining increases the water sorption in comparison to membranes with the same concentration of ZrPSPP particles fabricated without the electric field. The ZrPSPP/PVdF membranes have higher water sorption than Nafion/PVdF composites with the same fraction of proton conducting particles. The differences in water uptake between ZrPSPP and Nafion are like due to the higher hydrophilicity of ZrPSPP particles and the capillary filling of open spaces between the phases observed in Fig. 4(c) and (d). In both Nafion/PVdF and ZrPSPP/PVdF composite membranes, the

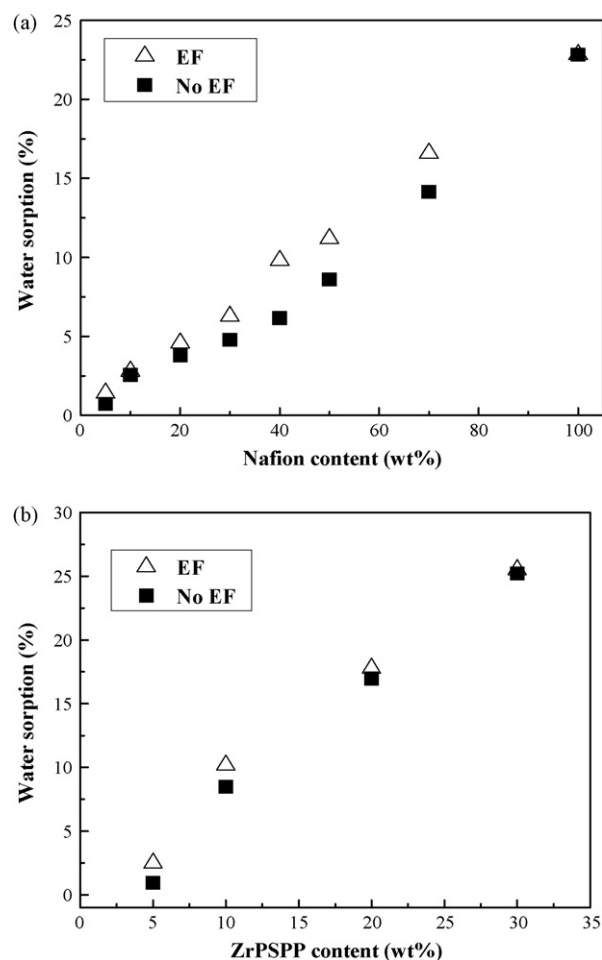
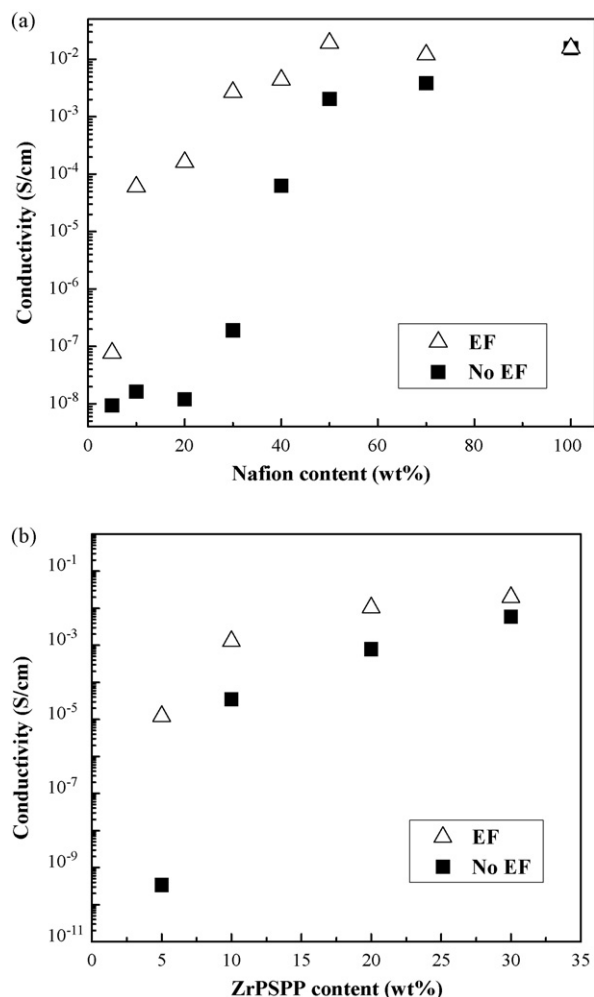


Fig. 5. Water sorption of composite membranes as a function of particle content and electric field processing: (a) Nafion/PVdF membranes, and (b) ZrPSPP/PVdF membranes.

water sorption of the membranes prepared with and without the applied field approaches similar values as the particle concentration increases. If particle concentration is increased high enough, the percolation threshold is reached at which there is good connectivity among particles even if they are randomly distributed.

### 3.5. Membrane proton conductivity

The effect of the applied electric field on the proton conductivity was investigated for a series of membranes with varying Nafion or ZrPSPP particle concentration as shown in Fig. 6(a) and (b). There is obvious improvement of the proton conductivity for membranes formed under the electric field as compared to membranes formed without the applied field, particularly when the concentration of particles is low. This is due to the continuous contact among conductive particles when aligned by the electric field. Without the electric field, the particles form fewer continuous channels for proton transport across the membrane. For Nafion, increasing particle concentration to 30 wt% and 40 wt% results in increased proton conductivity of the membrane formed without the electric field, but the conductivity is still much lower than the membrane prepared with the electric field. Further increase of the Nafion particle concentration to 50 wt% and 70 wt%, results in significant increase in the proton conductivity of the membranes formed without the electric field so that the conductivity approaches that of the membranes with field-aligned particles. Above the percolation threshold, the



**Fig. 6.** Proton conductivity of composite membranes as a function of the particle content and electric field processing: (a) Nafion/PVdF membranes, and (b) ZrPSPP/PVdF membranes.

randomly distributed particles begin to form an interconnected network that provides conduction pathways through the membrane. Obviously, the structure induced by the applied field causes the percolation threshold to be reduced a factor of two or three for Nafion particles, so that electric field processed membranes can exhibit high proton conductivity with much lower concentration of the proton conducting component than is required for randomly structured composites.

In comparison to Nafion/PVdF membranes, the ZrPSPP/PVdF membranes show improvement in proton conductivity at a much lower particle concentration (5 wt%), as shown in Fig. 6(b). The enhancement at lower particle concentrations can be explained by considering the smaller particle size for ZrPSPP compared to Nafion, as shown in Fig. 1(a) and (b). Assuming Nafion and ZrPSPP have similar density, the same mass fraction of Nafion and ZrPSPP particles will occupy the same volume fraction. However, there will be a much higher number of ZrPSPP particles than Nafion particles of the same mass. If the particles are arranged in separate monolithic columns, each having a length equal to the membrane thickness, ZrPSPP forms a much higher number of chains through the composite membranes than Nafion [17]. As a result, the particle percolation threshold decreases significantly for the electric field oriented ZrPSPP/PVdF composite membranes. This illustrates the potential to fabricate conductive composite membranes with much lower par-

ticle concentration by scaling down the particle size. However, it should be pointed out that the field strength required to execute particle chaining will be much higher for smaller particles, as predicted by Eq. (1). Another reason for the higher conductivity of ZrPSPP/PVdF membranes compared to Nafion/PVdF with the same loading of proton conductive particles may be the higher conductivity of ZrPSPP particles. The ion exchange capacity (IEC) of Nafion is 0.91 mequiv./g [35]. The IEC of ZrPSPP was found by acid-base titration to be 3.4 mequiv./g on basis of both  $\text{-HPO}_4$  and  $\text{-SO}_3\text{H}$  groups and 1.7 mequiv./g on basis of the  $\text{-SO}_3\text{H}$  group alone. The higher IEC value of ZrPSPP compared to Nafion may be another factor causing higher proton conductivity of ZrPSPP/PVdF composite membranes.

### 3.6. Methanol permeability and membrane selectivity

The effect of particle chaining on the methanol permeability through the Nafion/PVdF and ZrPSPP/PVdF composite membranes is shown in Fig. 7(a) and (b). As expected, the methanol permeability decreases with increasing PVdF content in the composite membranes since the PVdF phase is an excellent methanol barrier. The membranes with particles aligned by the electric field have higher methanol permeability than membranes containing the same volume fraction of randomly distributed particles. This is consistent with the proton conductivity data since the particle chains formed under the electric field provide transport pathways

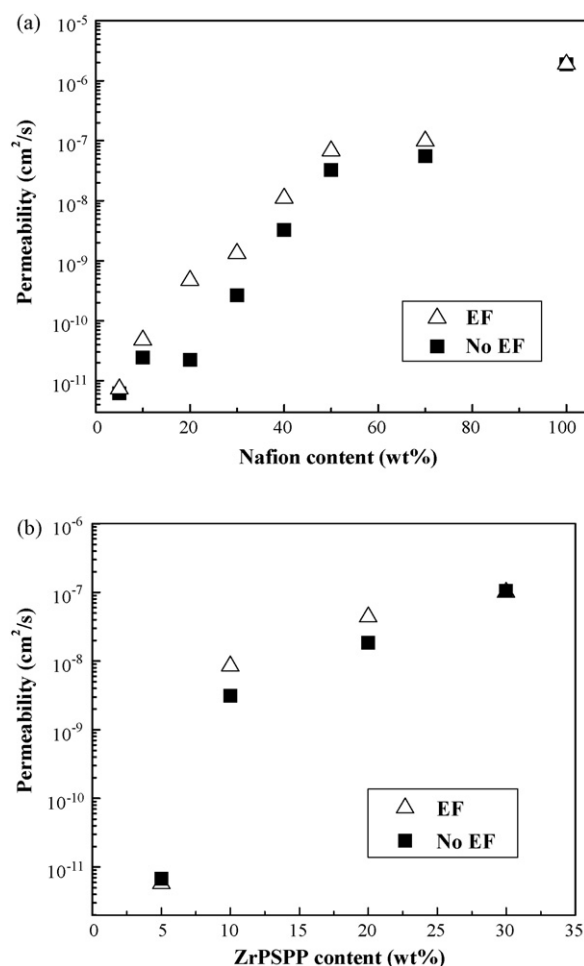


**Fig. 7.** Methanol permeability of composite membranes as a function of particle content and electric field processing: (a) Nafion/PVdF membranes, and (b) ZrPSPP/PVdF membranes.

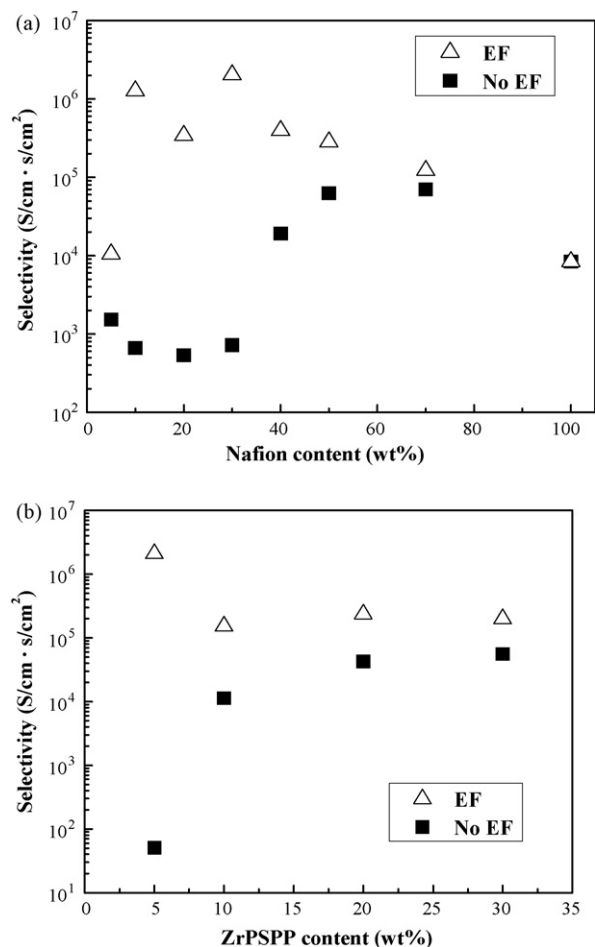


**Fig. 8.** Proton/methanol selectivity of the composite membranes as a function of particle content and electric field processing: (a) Nafion/PVdF membranes, and (b) ZrPSPP/PVdF membranes.

for protons as well as methanol. The selectivity ( $\alpha$ ) of the composite membranes for protons over methanol can be defined as the proton conductivity divided by the methanol permeability:  $\alpha = \sigma / P_m$  [30,36]. Fig. 8(a) and (b) shows the selectivity of the composite membranes fabricated with and without an applied electric field. The composite membranes formed under the electric field have an enhanced selectivity at particle concentrations below the percolation threshold for conductivity. At some concentrations below the percolation threshold, electric field induced particle alignment results in a huge enhancement in proton conductivity while the methanol permeability increases only slightly relative to disordered membranes. The differences in membrane selectivity between composite membranes with aligned and non-aligned particles are reduced after the particles reach the percolation concentration. The enhanced selectivity may be due to the suppressed swelling of Nafion or ZrPSPP phase by confinement in the PVdF matrix. Studies of structured composite membranes consisting of swellable methanol permeable material filled inside small pores of a rigid nonpermeable substrate have shown that swelling was constrained by confinement in the rigid pores and, as a result, methanol permeation was reduced [8,37].

### 3.7. Dimensional stability

Fig. 9(a) and (b) shows the measured changes in membrane area between the dry and water saturated states. As the Nafion con-

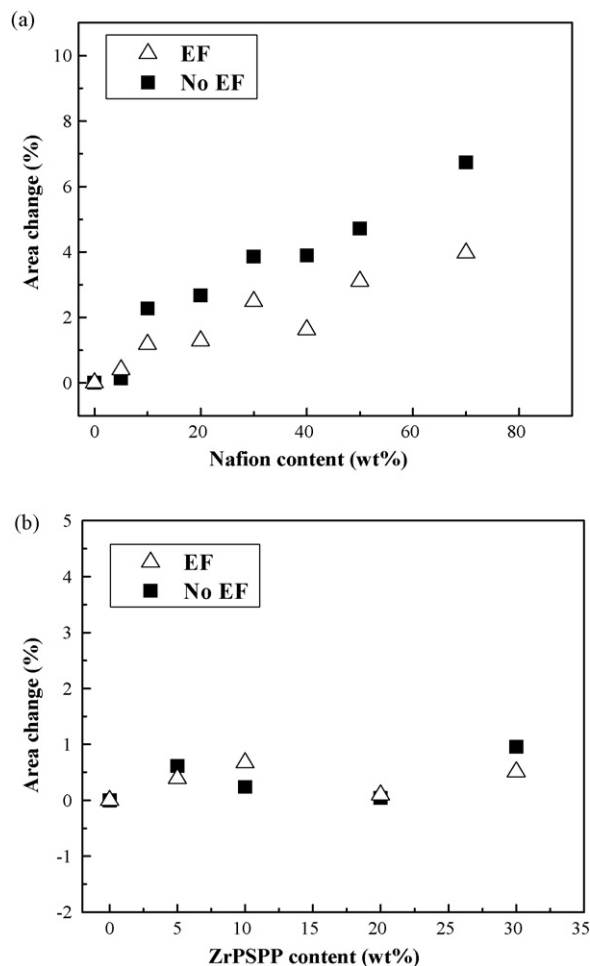


**Fig. 9.** Change in surface area of the composite membranes upon swelling with water as a function of particle content and electric field processing: (a) Nafion/PVdF membranes, and (b) ZrPSPP/PVdF membranes.

centration is increased, the membrane swelling increases for composite membranes with both aligned and non-aligned particles, as shown in Fig. 9(a). A pure Nafion115 membrane had a measured 22% increase in surface area due to swelling. All of the composite membranes displayed reduced swelling relative to pure Nafion. However, for composite membranes with the same particle content, the area expansion is reduced when the Nafion particles are aligned in chains. The water swelling behavior is important for practical operation of proton conducting membranes in fuel cells, and especially under humidity cycling. Electrodes can detach from a membrane surface due to the large membrane area change, because a carbon electrode does not swell with the membrane, leading to mechanical stress [8,9]. Composite membranes containing aligned particles fabricated by the present approach can effectively reduce the membrane area expansion. Electric field processing is therefore promising as a route to produce membranes with improved mechanical stability under humidity cycling in fuel cell applications.

Fig. 9(b) shows the dimensional changes due to water swelling for ZrPSPP/PVdF composite membranes. The area changes are quite small since the inorganic hydrophilic phase ZrPSPP does not swell significantly when exposed to water. As a result, the differences in the changes in membrane area between the field-processed and non-processed membranes are hard to compare because the slight dimensional changes are difficult to measure. Fig. 9(b) shows that all the fabricated ZrPSPP/PVdF composite membranes have little

water swelling in comparison to Nafion/PVdF membranes, pure Nafion or other ionomer based fuel cell membranes [38]. The fact that the ZrPSPP/PVdF membranes display limited swelling even though their water uptake is greater than Nafion/PVdF membranes suggests much of the water uptake in these membranes is into the interstitial regions between the two phases that were observed in Fig. 4. This limited swelling behavior may benefit the mechanical stability of the membranes or membrane electrode assemblies in operating fuel cells, provided the ZrPSPP particles remain intact during operation.

#### 4. Conclusions

The results confirm the theoretical prediction that proton conducting Nafion or ZrPSPP particles will selectively respond to an applied electric field when in a mixed suspension with PVdF particles. The applied field directs Nafion or ZrPSPP particles into chains that grow to span the gap between electrodes as the electric field is applied. By removing solvent and melting the PVdF phase under the applied field, composite membranes were formed with improved transport properties. The structure induced by the applied field enhances the proton conductivity and water uptake of the composite membranes. Membranes formed under the applied field display improved selectivity for protons over methanol due to the suppressed swelling of Nafion or ZrPSPP particles by PVdF.

The present study shows the promise of the novel electric field processing technique for the development of PVdF composite membranes that would display improved performance in direct methanol fuel cells. The applied field allows the morphology of the proton conducting phase to be adjusted in order to balance proton conductivity, methanol permeability and mechanical stability. The cell used in the present study produced membranes with thickness around 800  $\mu\text{m}$ , which limits application in actual fuel cells due to the high ohmic resistance of the thick membranes. Future study will focus on the reduction of the membrane thickness to 150  $\mu\text{m}$  or less in order to reduce the ohmic resistance and allow practical application in DMFCs.

#### Acknowledgments

We acknowledge support from the DOE (DE-FG02-05ER15722) and the DOE through the Laboratory for Laser Energetics (DE-FC03-92SF19460) for support of this research.

#### Nomenclature

$E$	applied field strength (V/mm)
$K_B$	Boltzmann's constant (J/K)
$P_m$	methanol permeability ( $\text{cm}^2/\text{s}$ )
$r$	radius of the particle (m)
$T$	absolute temperature (K)
$\alpha$	membrane selectivity ( $\text{S}/\text{cm s}/\text{cm}^2$ )
$\beta$	particle dipole coefficient
$\epsilon_i$	relative permittivity of the solvent or particle
$\epsilon_0$	permittivity of free space (F/m)
$\epsilon_1$	relative permittivity of the solvent
$\lambda$	relative strengths of the polarization forces and Brownian motion
$\sigma$	proton conductivity ( $\text{S}/\text{cm}$ )
$\sigma_i$	conductivity of the particle or solvent ( $\text{S}/\text{m}$ )
$\sigma_1$	conductivity of the solvent ( $\text{S}/\text{m}$ )
$\sigma_2$	conductivity of the particle ( $\text{S}/\text{m}$ )

#### References

- [1] J. Ge, H. Liu, Experimental studies of a direct methanol fuel cell, *J. Power Sources* 142 (2005) 56–69.
- [2] M. Waidhas, W. Drenckhahn, W. Preidel, H. Landes, Direct-fueled fuel cells, *J. Power Sources* 61 (1996) 91–97.
- [3] V. Neburchilov, J. Martin, H. Wang, J. Zhang, A review of polymer electrolyte membranes for direct methanol fuel cells, *J. Power Sources* 169 (2007) 221–228.
- [4] N.W. Delucla, Y.A. Elabd, Polymer electrolyte membranes for the direct methanol fuel cell: a review, *J. Polym. Sci. B: Polym. Phys.* 44 (2006) 2201–2225.
- [5] A. Heinzel, V.M. Barragan, A review of the state-of-the-art of the methanol crossover in direct methanol fuel cells, *J. Power Sources* 84 (1999) 70–74.
- [6] S. Hikita, K. Yamane, Y. Nakajima, Measurement of methanol crossover in direct methanol fuel cell, *JSME Rev.* 22 (2001) 151–156.
- [7] G. Alberti, M. Casciola, Solid state protonic conductors, present main applications and future prospects, *Solid State Ionics* 145 (2001) 3–16.
- [8] T. Yamaguchi, F. Miyata, S.-I. Nakao, Polymer electrolyte membranes with a pore-filling structure for a direct methanol fuel cell, *Adv. Mater.* 15 (2003) 1198–1201.
- [9] T. Yamaguchi, F. Miyata, S.-I. Nakao, Pore-filling polymer electrolyte membranes for a direct methanol fuel cell, *J. Membr. Sci.* 214 (2003) 283–292.
- [10] Y.-S. Park, Y. Yamazaki, Novel Nafion/hydroxyapatite composite membrane with high crystallinity and low methanol crossover for DMFCs, *Polym. Bull.* 53 (2005) 181–192.
- [11] K.D. Kreuer, On the development of proton conducting polymer membranes for hydrogen and methanol fuel cells, *J. Membr. Sci.* 185 (2001) 29–39.
- [12] G. Alberti, M. Casciola, U. Costantino, Protonic conductivity of layered zirconium phosphonates containing  $-\text{SO}_3\text{H}$  groups. I. Preparation and characterization of a mixed zirconium phosphonate of composition  $\text{Zr}(\text{O}_3\text{PR})_{0.73}(\text{O}_3\text{PR}')_{1.27} \cdot n\text{H}_2\text{O}$ , with  $\text{R} = -\text{C}_6\text{H}_4-\text{SO}_3\text{H}$  and  $\text{R}' = -\text{CH}_2-\text{OH}$ , *Solid State Ionics* 50 (1992) 315–322.
- [13] G. Alberti, M. Casciola, R. Palombi, Protonic conductivity of layered zirconium phosphonates containing  $-\text{SO}_3\text{H}$  groups. II. AC conductivity of zirconium alkyl-sulphophenyl phosphonates in the range 100–200 °C, in the presence or absence of water vapour, *Solid State Ionics* 58 (1992) 339–344.
- [14] G. Alberti, L. Boccali, M. Casciola, L. Massinelli, E. Montoneri, Protonic conductivity of layered zirconium phosphonates containing  $-\text{SO}_3\text{H}$  groups. III. Preparation and characterization of r-zirconium sulfoaryl phosphonates, *Solid State Ionics* 84 (1996) 97–104.
- [15] M. Casciola, G. Alberti, A. Ciarletta, A. Cruccolini, P. Piaggio, M. Pica, Nanocomposite membranes made of zirconium phosphate sulphonylenephosphonate dispersed in polyvinylidene fluoride: preparation and proton conductivity, *Solid State Ionics* 176 (2005) 2985–2989.
- [16] J.-C. Lin, M. Ouyang, J.M. Fenton, H.R. Kunz, J.T. Koberstein, M.B. Cutlip, Study of blend membranes consisting of Nafion and vinylidene fluoride-hexafluoropropylene copolymer, *J. Appl. Polym. Sci.* 70 (1998) 121–127.
- [17] Y. Oren, V. Freger, C. Linder, Highly conductive ordered heterogeneous ion-exchange membranes, *J. Membr. Sci.* 239 (2004) 17–26.
- [18] S.B. Brijmohan, M.T. Shaw, Magnetic ion-exchange nanoparticles and their application in proton exchange membranes, *J. Membr. Sci.* 303 (2007) 64–71.
- [19] T. Arimura, D. Ostrovskii, T. Okada, G. Xie, The effect of additives on the ionic conductivity performances of perfluoroalkyl sulfonated ionomer membranes, *Solid State Ionics* 118 (1999) 1–10.
- [20] T.B. Jones, *Electromechanics of Particles*, Cambridge University Press, Cambridge, 1995.
- [21] M. Parthasarathy, D.J. Klingenberg, Electrorheology: mechanisms and models, *Mater. Sci. Eng. R* 17 (1996) 57–103.
- [22] D. Liu, M.Z. Yates, Tailoring the structure of S-PEEK/PDMS proton conductive membranes through applied electric fields, *J. Membr. Sci.* 322 (2008) 256–264.
- [23] T. Kyu, J.-C. Yang, Miscibility studies of perfluorinated nafion ionomer and poly(vinylidene fluoride) blends, *Macromolecules* 23 (1990) 176–182.
- [24] M.-K. Song, Y.-T. Kim, J.M. Fenton, H.-W. Rhee, K.H. Russell, Chemically-modified Nafion/poly(vinylidene fluoride) blend ionomers for proton exchange membrane fuel cells, *J. Power Sources* 117 (2003) 14–21.
- [25] J.L. Garcia, K.W. Koelling, R.R. Seghi, Mechanical and wear properties of polymethylmethacrylate and polyvinylidene fluoride blends, *Polymer* 39 (1998) 1559–1567.
- [26] W.-K. Lee, C.-S. Ha, Miscibility and surface crystal morphology of blends containing poly(vinylidene fluoride) by atomic force microscopy, *Polymer* 39 (1998) 7131–7134.
- [27] G. Alberti, M. Casciola, A. Donnadio, P. Piaggio, M. Pica, M. Sisani, Preparation and characterisation of  $\alpha$ -layered zirconium phosphate sulphonylenephosphonates with variable concentration of sulfonic groups, *Solid State Ionics* 176 (2005) 2893–2898.
- [28] E. Montoneri, M.C. Gallazzi, M. Grassi, Organosulphur phosphorus acid compounds. Part 1. *m*-Sulphophenylphosphonic acid, *J. Chem. Soc., Dalton Trans.* (1989) 1819–1823.
- [29] J. Crank, *The Mathematics of Diffusion*, Oxford University Press, Oxford, 1975.
- [30] Y.A. Elabd, E. Napadensky, J.M. Sloan, D.M. Crawford, C.W. Walker, Triblock copolymer ionomer membranes part I: methanol and proton transport, *J. Membr. Sci.* 217 (2003) 227–242.
- [31] H. Morgan, N.G. Green, *AC Electrokinetics: Colloids and Nanoparticles*, Research Studies Press LTD, Baldock, 2003.
- [32] A.P. Gast, C.F. Zukoski, Electrorheological fluids as colloidal suspensions, *Adv. Colloid Interf. Sci.* 30 (1989) 153–202.

- [33] C. Gehin, G. Persello, D. Charraut, B. Cabane, Electrorheological properties and microstructure of silica suspensions, *J. Colloid Interf. Sci.* 273 (2004) 658–667.
- [34] B. Liu, S.A. Boggs, M.T. Shaw, Electrorheological properties of anisotropically filled elastomers, *IEEE Trans. Dielectr. Electr. Insul.* 8 (2001) 173–181.
- [35] S.-L. Chen, A.B. Bocarsly, J. Benziger, Nafion-layered sulfonated polysulfone fuel cell membranes, *J. Power Sources* 152 (2005) 27–33.
- [36] B. Libby, W.H. Smyrl, E.L. Cussler, Polymer-zeolite composite membranes for direct methanol fuel cells, *AIChE J.* 49 (2003) 991–1001.
- [37] H. Munakata, D. Yamamoto, K. Kanamura, Properties of composite proton-conducting membranes prepared from three-dimensionally ordered macroporous polyimide matrix and polyelectrolyte, *Chem. Commun.* (2005) 3986–3988.
- [38] M.B. Satterfield, P.W. Majsztzik, H. Ota, J.B. Benziger, A.B. Bocarsly, Mechanical properties of Nafion and titania/Nafion composite membranes for polymer electrolyte membrane fuel cells, *J. Polym. Sci. B: Polym. Phys.* 14 (2006) 2327–2345.